A Search for Invariant Relative Satellite Motion

Authors: J.D. Biggs, V.M. Becerra, S.J. Nasuto, V.F. Ruiz, W. Holderbaum
Contractor: Department of Cybernetics, The University of Reading

Technical officer: Dario Izzo, Advanced Concepts Team (ESA/ESTEC)

Contacts:

Dario Izzo
Tel: ++31 (0)71565 – 3511
Fax: ++31 (0)71565 – 8018
e-mail: act@esa.int

Ariadna id: 04/4104
Study length: 4 months.
Contract Number: 18875/05/NL/MV

Abstract

This report presents the canonical Hamiltonian formulation of relative satellite motion. The unperturbed Hamiltonian model is shown to be equivalent to the well known Hill-Clohessy-Wilshire (HCW) linear formulation. The influence of perturbations of the nonlinear Gravitational potential and the oblateness of the Earth; J_2 perturbations are also modelled within the Hamiltonian formulation. The modelling incorporates eccentricity of the reference orbit. The corresponding Hamiltonian vector fields are computed and implemented in Simulink. A numerical method is presented aimed at locating periodic or quasi-periodic relative satellite motion. The numerical method outlined in this paper is applied to the Hamiltonian system. Although the orbits considered here are weakly unstable at best, in the case of eccentricity only, the method finds exact periodic orbits. When other perturbations such as nonlinear gravitational terms are added, drift is significantly reduced and in the case of the J_2 perturbation with and without the nonlinear gravitational potential term, bounded quasi-periodic solutions are found. Advantages of using Newton's method to search for periodic or quasi-periodic relative satellite motion include simplicity of implementation, repeatability of solutions due to its non-random nature, and fast convergence.

Given that the use of bounded or drifting trajectories as control references carries practical difficulties over long-term missions, Principal Component Analysis (PCA) is applied to the quasi-periodic or slowly drifting trajectories to help provide a closed reference trajectory for the implementation of closed loop control.

In order to evaluate the effect of the quality of the model used to generate the periodic reference trajectory, a study involving closed loop control of a simulated master/follower formation was performed.

The results of the closed loop control study indicate that the quality of the model employed for generating the reference trajectory used for control purposes has an important influence on the resulting amount of fuel required to track the reference trajectory. The model used to generate LQR controller gains also has an effect on the efficiency of the controller.

Contents

1 Introduction

There has been a considerable interest in using clusters of small cooperative satellites to perform multi-tasks as opposed to a single large expensive satellite. A cluster of satellites will be able to synthesize a much larger aperture for Earth mapping interferometry than can be achieved with a single platform. Accurate modelling of relative motion dynamics for initial conditions close to the leader satellite is essential for this problem. Therefore, the solutions of interest are restricted to a specific set of initial conditions that lead to periodic motion, such that the satellites do not drift apart. The celebrated Clohessy-Wiltshire (CW) equations (see [1]) describe the relative motion of one satellite with respect to another under the assumptions of a circular reference orbit, spherical earth and linearized gravitational potential. These equations of relative motion can be solved explicitly and a constraint on the initial conditions can be calculated which generate periodic motion. However, these initial conditions have to be corrected to obtain bounded solutions in the presence of nonlinearity in the gravitational potential, the oblateness of the Earth, and eccentricity of the reference orbit; the three most important perturbations that break down the periodic orbit solutions of the CW equations, see reference [2].

There is a wealth of literature on this problem and mentioned here are some of the most recent papers. Inalhan, Tillerson and How [4] derive explicit solutions of the linearized relative equations of motion with eccentricity of the reference orbit and find necessary conditions on the initial states that produce periodic solutions. Reference [5] studies the effects of J_2 perturbations and air drag which induce secular effects, i.e. a drift of relative position and implements an impulsive velocity correction control to compensate for this drift. In [6], Shaub and Alfriend, defined J_2 invariant orbits by developing special relationships between the deviations of the mean orbital elements and developed nonlinear control laws to establish these orbits. In [7], Wiesel, proposes a Hamiltonian formulation, which has the advantage of the ease of adding perturbations and considers the oblateness of the Earth and air drag. In this model the solution conceptually resembles the CW solution for relative motion, but includes all zonal harmonics of the Earth's gravitational field. This paper includes all gravitational harmonics through order 14, and uses Floquet theory to find periodic solutions. There is little work done which considers the combined effects of the nonlinearity in the gravitational potential, the oblateness of the Earth and eccentricity. This report describes a variant of Newton's method aimed at locating periodic or quasi-periodic relative satellite motion. The original method, which is based on the Hamiltonian formalism, has been proposed for locating periodic orbits embedded in a largely chaotic system [9, 12]. In the original method, segments characterized by a relatively low positive local Lyapunov exponent which characterize stable orbits are located. Once this selection is made convergence to stable (or weakly unstable) periodic orbits is obtained by Newton's method.

The Newton method was applied to the Hamiltonian model of relative motion. In the unperturbed case an analytic condition is observed (equivalent to the well known Clohessy-Wiltshire equations) that gives a closed periodic solution. As perturbations are added this condition no longer gives closed solutions, but does however serve as a good initial guess for the application of Newton's method. Finally, a closed loop controller is applied to the relative satellite motion model, using the trajectories found using the Newton method, as reference orbits.

2 Methodology

It is proposed that as many nonlinearities as possible are taken into consideration in the 'study model'. The study model consists of the Hamiltonian equations of motion that include the conservative perturbations; nonlinear gravitational potential terms, zonal harmonics and eccentricity. The study uses a numerical method for locating periodic solutions embedded in a largely chaotic system, see reference [9] which is applied to the study model outlined in this report. One of the assumptions of this method is that it is implemented in the Hamiltonian formalism, it is also necessary to compute trajectories and it is therefore necessary to derive the Hamiltonian equations of motion.

In a recent paper, [8], Kasdin and Gurfill present a Hamiltonian approach to modelling relative spacecraft motion based on the derivation of canonical coordinates. The Hamiltonian formulation accommodates the modelling of nonlinear terms and orbital perturbations via variation of parameters. Kasdin and Gurfil derive the kinetic and potential energy of the system in order to define the Lagrangian function (function on a vector space) and use the Legendre transformation to construct the Hamiltonian function (function on the dual space). The formulation used in this report is the same as in [8] except that the nonlinear model is used rather than truncations of the perturbation terms and the normalization of the gravitational constant, the radius of the reference satellite about the Earth and mean motion are not assumed. This is the most suitable coordinate system for our purposes as the unperturbed Hamiltonian is shown to be equivalent to the CW equations and the perturbations can be added easily, thus adding complexity in a stepwise manner. In addition this coordinate system allows the use of control and simulation techniques to be implemented effectively.

The ‘study model’ is used to obtain initial conditions that induce periodic or quasi-periodic orbits. It includes various perturbations of relevance including eccentricity, gravitational nonlinearities and zonal harmonics. Once these orbits have been found for the model with the most complexity, they are used as reference orbits in closed loop control simulations involving the ’full model’. The full model includes nonlinearities, eccentricity, the J_2 perturbation and actuation variables for the implementation of closed loop control.
To implement the variant of the Newton method it is necessary to compute the Hamiltonian function and the corresponding Hamiltonian vector fields, the latter are computed with the aid of Mathematica. The Hamiltonian equations of motion, which were implemented in Simulink, are derived and expressed in the Appendix.

3 Hamiltonian Formulation

3.1 Deriving the Lagrangian

The Hamiltonian formulation has many advantages. Firstly, for our purposes it allows the Newton method to be applied, as this method relies on the conserved energy constraint given by the Hamiltonian function. In addition the Hamiltonian formulation allows for additional conservative forces to be added to the Hamiltonian, thus the addition of complexity to the model can be incorporated with ease. Nonconservative forces can be added in the momenta equations of motion. The Hamiltonian equations of motion allows us to directly use control and simulation techniques. Inspired by [8] we derive the Hamiltonian function equivalent to the HCW equations and then derive the nonlinear equations of motion which will be used to search for periodic or quasi-periodic orbits. The Hamiltonian equations of motion are then derived with the aid of Mathematica. The coordinate system (a rotating Cartesian Euler-Hill system see Figure 1), denoted by $\Re$, is defined by the unit vectors

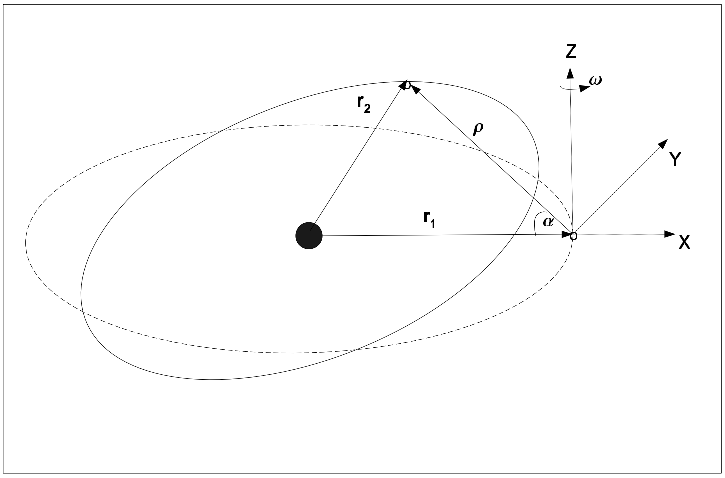

Figure 1: Euler-Hill Reference frame - Relative motion

$\hat{x}, \hat{y}, \hat{z}$. In [8] the equations of motion are derived on a circular reference orbit of radius a about the Earth. The co-ordinate system is rotating with frequency $\omega = \sqrt{\mu/a^3}$, where μ is the gravitational constant. However, in the following derivation the reference orbit is not restricted to a circle in order to account for the effect of eccentricity. The radius is denoted r and the rate of change of the true anomaly is denoted $\dot{\theta}$. The reference orbit plane is the fundamental plane, the positive $\hat{x}-$ axis points radially outward , the $\hat{y}-$ axis is the relative position in the cross track direction, and the $\hat{z}-$ axis is orthonormal to both $\hat{x}$ and $\hat{y}$ and is out of the leader satellite plane. The first step is to derive the Lagrangian of relative motion. The velocity of the follower satellite is given by:

$$\vec{v} = {}^{\Im}\vec{\omega}^{\Re} \times \vec{r}_1 + \frac{d^{\Re}}{dt}\vec{\rho} + {}^{\Im}\vec{\omega}^{\Re} \times \vec{\rho} \tag{3.1}$$

where $\vec{r}_1 \in \mathbb{R}^3$ is the inertial position vector of the leader satellite along the reference orbit, $\vec{\rho} = [x, y, z]^T$ is the relative position vector in the rotating frame, and ${}^{\Im}\vec{\omega}^{\Re} = [0, 0, n]^T$ is the angular velocity of the rotating frame $\Re$ with respect to the inertial frame $\Im$. Denoting $\|\vec{r}_1\| = r$ and substituting into (3.1) in componentwise notation:

$$\vec{v} = \begin{bmatrix} \dot{x} - \omega y + \dot{r} \\ \dot{y} + \omega x + \omega r \\ \dot{z} \end{bmatrix} \tag{3.2}$$

The kinetic energy per unit mass is given by

$$K = \frac{1}{2}\|\vec{v}\|^2 \tag{3.3}$$

Initially assuming a spherical attracting Earth, the potential energy of the follower satellite, whose position vector is $\vec{r}_2$, is the usual gravitational potential written in terms of $\rho = \|\vec{\rho}\|$ and expanded using Legendre polynomials.

$$\begin{aligned} U &= -\frac{\mu}{\|\vec{r}_2\|} = -\frac{\mu}{\|\vec{r}_1 + \vec{\rho}\|} = -\frac{\mu}{r\left[1 + 2\frac{\vec{r}_1 \cdot \vec{\rho}}{r^2} + \left(\frac{\rho}{r}\right)^2\right]^{1/2}} \\ &= -\frac{\mu}{r}\sum_{k=0}^{\infty} P_k(\cos\alpha)\left(\frac{\rho}{r}\right)^k \end{aligned} \tag{3.4}$$

where the $P_k(\cos\alpha)$ are the Legendre polynomials,

$$\cos\alpha = \frac{\vec{\rho} \cdot \vec{r}}{r\rho} = \frac{-x}{\rho} \tag{3.5}$$

and α is the angle between $\vec{r}_1$ and the relative position vector $\vec{\rho}$. The Lagrangian $\mathfrak{L}$ is then equal to $K - U$:

$$\mathfrak{L}^{(0)} = \frac{1}{2}\{\dot{x} - \dot{\theta}y + \dot{r})^2 + (r\dot{\theta} + \dot{\theta}x + \dot{y})^2 + \dot{z}\} + \frac{\mu}{r}\sum_{k=0}^{\infty} P_k(\cos\alpha)\left(\frac{\rho}{r}\right)^k \tag{3.6}$$

Using Legendre polynomials up to $k = 3$ and substituting (3.5) into (3.6) the following Lagrangian is obtained:

$$\mathfrak{L}^{(0)} = \frac{1}{2}((\dot{x} - \dot{\theta}y + \dot{r})^2 + (r\dot{\theta} + \dot{\theta}x + \dot{y})^2 + \dot{z} + \frac{\mu}{r} - \frac{\mu x}{r^2} + \frac{3\mu x^2}{2r^3} - \frac{\mu(x^2 + y^2 + z^2)}{2r^3}) \tag{3.7}$$

In [8], Kasdin and Gurfil, proceed using simplifying calculations by taking a normalization of $\dot{\theta}$ and r, here we proceed and calculate the Hamiltonian without normalization.

3.2 Deriving the Hamiltonian Vector Fields

To calculate the Hamiltonian for the Cartesian system first derive the canonical momenta from the Lagrangian $\mathfrak{L}^{(0)}$:

$$\begin{aligned} p_x &= \frac{\partial \mathfrak{L}^{(0)}}{\partial \dot{x}} = \dot{x} - \omega y + \dot{r} \\ p_y &= \frac{\partial \mathfrak{L}^{(0)}}{\partial \dot{y}} = \dot{y} + \omega(r + x) \\ p_z &= \frac{\partial \mathfrak{L}^{(0)}}{\partial \dot{z}} = \dot{z} \end{aligned} \tag{3.8}$$

then using the Legendre transformation $H = \sum \dot{q}_i p_i - \mathfrak{L}$ the Hamiltonian corresponding to the Clohessy-Wiltshire (CW) equations, called the unperturbed Hamiltonian is given by:

$$H^{(0)} = \sum \dot{q}_i p_i - \mathfrak{L}^{(0)} \tag{3.9}$$

Therefore, the Hamiltonian function is:

$$\begin{aligned} H^{(0)} =& \frac{1}{2}(-p_x^2 - p_y^2 + p_z^2 + 2p_y(p_y - r\dot{\theta} - \dot{\theta}x) + 2p_x(p_x - \dot{r} + \dot{\theta}y) \\ &+ \frac{2\mu}{r} + \frac{2\mu x}{r^2} - \frac{3\mu x^2}{r^3} + \frac{\mu(x^2 + y^2 + z^2)}{r^3}) \end{aligned} \tag{3.10}$$

From the Hamiltonian function, which is itself an integral of motion, the Hamiltonian vector fields can be calculated using Hamilton's canonical equations:

$$\begin{aligned} \dot{q}_i &= \frac{\partial H}{\partial p_i} \\ \dot{p}_i &= -\frac{\partial H}{\partial q_i} \end{aligned} \tag{3.11}$$

where $q \in \mathbb{R}^3$ are the degrees of freedom in the configuration space and $p \in \mathbb{R}^3$ is the conjugate momenta. Calculating the corresponding Hamiltonian vector fields yields:

$$
\begin{aligned}
\dot{x} &= p_x + \omega y - \dot{r} \\
\dot{y} &= p_y - \omega(r + x) \\
\dot{z} &= p_z \\
\dot{p}_x &= -\frac{\mu}{r^2} + \frac{2\mu x}{r^3} + p_y \dot{\theta} \\
\dot{p}_y &= -\frac{\mu y}{r^3} - p_x \dot{\theta} \\
\dot{p}_z &= -\frac{\mu z}{r^3}
\end{aligned}
\tag{3.12}
$$

These equations are equivalent to the well known HCW equations (with eccentricity of the reference orbit), see Appendix A for proof. In the CW equations, it is known that the constraint on the initial conditions $\dot{y}_0 = -2\omega x_0$ gives the desired periodic motion. Substituting this constraint into (3.8) gives the corresponding constraint for periodic motion in the Hamiltonian vector fields, $p_{y0} = \omega(a - x_0)$, which is verified to give periodic motion through simulation of the Hamiltonian equations of motion (see section 5). This derivation is useful (as with the HCW equations) can fit into well established linear control theory. However, unlike the classical HCW formulation the equations can account for non Keplarian forces by adding perturbations to the Hamiltonian. However, for the purposes of this work, it is necessary to derive the nonlinear Hamiltonian equations of motion. The nonlinear model gives significantly more accurate and precise results than the HCW model.

4 The Nonlinear Hamiltonian and perturbations

4.1 Nonlinear Gravitational Potential

Following the derivation in Section 3, but instead of computing the Legendre expansion in the gravitational potential equation (3.4), the nonlinear equations are obtained by writing:

$$\|\vec{r}_2\| = ((r+x)^2 + y^2 + z^2)^{1/2} \tag{4.1}$$

Then the Hamiltonian function is calculated as

$$H^{(0)} = -\frac{p_x^2}{2} - \frac{p_y^2}{2} + \frac{p_z^2}{2} + p_y(p_y - \dot{\theta}r - \dot{\theta}x) + p_x(p_x - \dot{r} + \dot{\theta}y) - \frac{\mu}{((r+x)^2 + y^2 + z^2)^{1/2}} \tag{4.2}$$

The corresponding Hamiltonian equations of motion derived with the aid of Mathematica are given in Appendix B.

4.2 Earth oblateness perturbations

In addition to the nonlinear gravitational potential, it is necessary to account for the zonal harmonics in the gravitational potential. The J2 harmonic is known to be the most significant. Assuming that the earth is axially symmetric, the external potential due to the gravitational zonal harmonics is given by [11]:

$$U = \sum_{k=2}^{\infty} U_k = -\frac{\mu}{\|\vec{r}_2\|} \sum_{k=2}^{\infty} J_k \left(\frac{R_e}{\|\vec{r}_2\|}\right)^k P_k(\cos\phi) \tag{4.3}$$

where ϕ is the follower spacecraft colatitude angle

$$\cos\phi = \frac{Z}{\|\vec{r}_2\|}, \tag{4.4}$$

Z is the normal deflection in an inertial, geocentric-equatorial reference frame and $J_k (k = 2, 3..)$ are constants of the zonal harmonics. Assuming that the reference orbit is not inclined relative to the equatorial plane, so that $Z = z$. Then the J_2 term only is represented by the equation:

$$U_{J_2} = -\frac{\mu J_2}{2\,\|r_2\|}\left(\frac{R_e}{\|r_2\|}\right)^2\left(3\frac{z^2}{\|r_2\|^2} - 1\right) \tag{4.5}$$

and substituting (4.6) into (4.5)

$$\|r_2\| = ((r + x)^2 + y^2 + z^2)^{1/2} \tag{4.6}$$

simplifying and rearranging gives

$$H^{(1)} = \frac{J_2 R_e^2 u(-(r + x)^2 - y^2 + 2z^2)}{2((r + x)^2 + y^2 + z^2)^{5/2}} \tag{4.7}$$

Eccentricity is accommodated into the model as r, $\dot{r}$ and $\dot{\theta}$ are dependent on the reference orbit which can be initialized with a particular eccentricity. This analysis extends to higher order zonal harmonics.

4.3 The reference orbit

Now that the study model is in place, it is necessary to define $\dot{\theta}$, r and $\dot{r}$ independently of the Hamiltonian system and treat them as inputs into the Simulink model. In the simple case of an unperturbed Keplarian orbit there are a number of ways to simulate the reference orbit. Using fundamental orbital mechanics describing planetary motion in a local vertical-local horizontal (LVLH) reference frame shown in Figure 2, where **E** is the eccentric anomaly and assuming that the zonal harmonics do not affect the reference orbit, the radius and angular velocity of the reference orbit can be written as

$$\begin{aligned} r &= \frac{a(1 - e^2)}{1 + e\cos\theta} \\ \dot{\theta} &= \frac{\omega(1 + e\cos\theta)^2}{(1 - e^2)^{3/2}} \end{aligned} \tag{4.8}$$

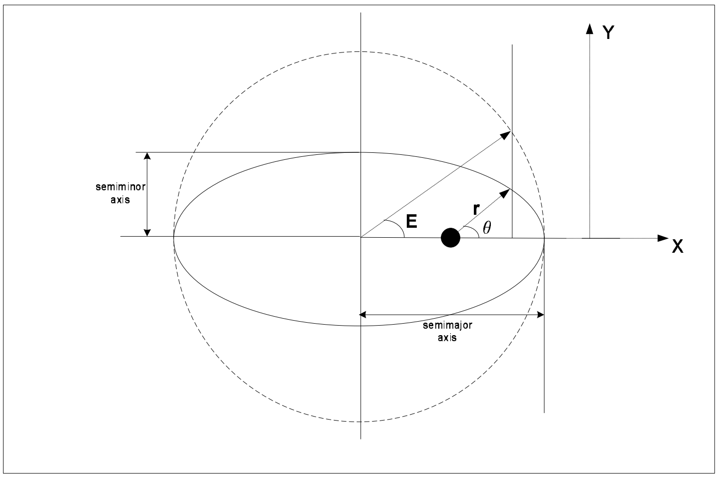

Figure 2: Equatorial plane, true and eccentric anomaly

This formulation was used in [4] in the context of relative motion with eccentricity. Although these equations cannot be solved analytically, it is possible to use a numerical integrator within the Simulink environment and then implement them as inputs into the Hamiltonian vector fields as the simulation is running. The advantage of this method is its simplicity in implementation. Another method used to calculate these input parameters is to numerically integrate Kepler's equation. The mean anomaly and its time derivative are denoted M and $\dot{M}$ respectively, the eccentric anomaly E is calculated using Kepler's equation, see [13]:

$$E = M + e \sin E \tag{4.9}$$

where e is the eccentricity of the reference orbit. However, this equation is transcendental in the eccentric anomaly E, thus no closed form solution for E is possible. Differentiating (4.9) yields

$$\dot{E} = \dot{M} + \dot{E} e \cos E \tag{4.10}$$

and rearranging gives

$$\dot{E} = \frac{\dot{M}}{(1 - e\cos E)} \tag{4.11}$$

This equation is then solved using a numerical integrator in SIMULINK, giving both $\dot{E}$ and E. The true anomaly v is then given by the equation:

$$\tan\left(\frac{v}{2}\right) = \sqrt{\frac{1+e}{1-e}}\tan\left(\frac{E}{2}\right) \tag{4.12}$$

and the radius r from:

$$r = \frac{a(1-e^2)}{1+e\cos v} \tag{4.13}$$

where $\dot{v}$ and $\dot{r}$ are calculated by the time derivatives of (4.12) and (12.12), respectively:

$$\dot{v} = \frac{2\sqrt{\frac{1+e}{1-e}}\dot{E}}{1 + \left(\frac{1+e}{1-e}\right) - \left(\left(\frac{1+e}{1-e}\right) - 1\right)\cos E} \tag{4.14}$$

$$\dot{r} = \sqrt{\frac{1+e}{1-e}}\frac{a(1-e^2)\dot{v}\sin v}{1+e\cos v} \tag{4.15}$$

The advantage of using this method is that the initial conditions are stated in terms of the orbital elements e, a and M. For perturbations to the reference orbit such as J_2, the nonlinear propagator STK was used to compute the the reference orbit time dependent variables.

5 Implementation in Simulink

The constants of motion are:

$$\begin{aligned} \mu &= 3.986005 \times 10^5 \text{ km}^3/\text{s}^2 \\ R_e &= 6378.140 \text{ km} \\ J_2 &= 0.00108263 \end{aligned} \tag{5.1}$$

The condition for periodic solutions in the CW equations are implemented into each model i.e. $p_{y_0} = \dot{\theta}_0(r_0 - x_0)$. Then setting the initial conditions as:

$$\begin{aligned}
x_0 &= 10 \text{ km} \\
y_0 &= 10 \text{ km} \\
z_0 &= 10 \text{ km} \\
p_{x_0} &= 0 \text{ kg m/s} \\
p_{y_0} &= \dot{\theta}_0(r_0 - x_0) \text{ kg m/s} \\
p_{z_0} &= 0 \text{ kg m/s}
\end{aligned} \tag{5.2}$$

with the reference orbit initialized at:

$$\begin{aligned}
r_0 &= 6700 \\
\dot{r}_0 &= 0 \\
\theta_0 &= 0 \\
\dot{\theta}_0 &= 0.001151213
\end{aligned} \tag{5.3}$$

These initial conditions give a closed orbit as shown in Figure 3 shows the relative motion for the Hamiltonian equations of motion. When perturbations are added to the linearized CW equations for the previous initial conditions the relative trajectory will drift. For the purposes of quantitative comparison of the different trajectories, the initial drift d_T was calculated when appropriate as follows:

$$d_T = \sqrt{(x(T) - x(0))^2 + (y(T) - y(0))^2 + (z(T) - z(0))^2} \tag{5.4}$$

where T is the approximate period, x is the radial distance, y is the along track distance and, z the out of plane distance. Notice, however, that the drift rate may change from orbit to orbit, and that a trajectory that initially appears to be drifting may actually be bounded. Introducing eccentricity

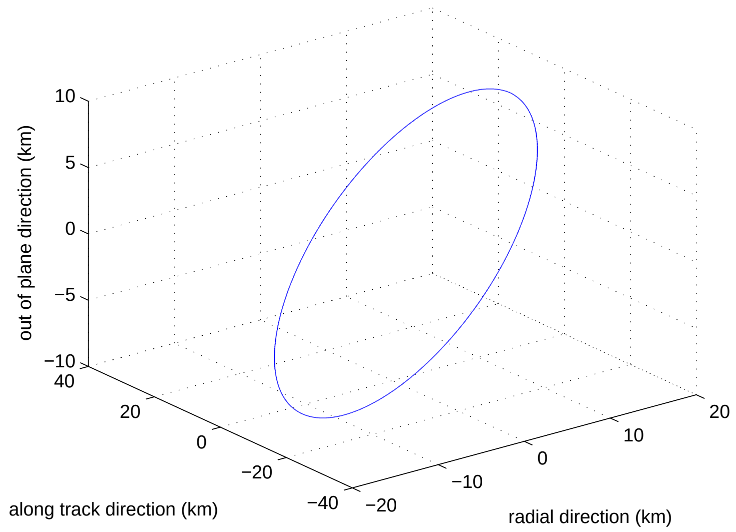

Figure 3: CW - Periodic solution for linearized $H^{(0)}$

of the reference orbit into the model where $e = 0.005$ and $a = 6700km$, initializes the reference orbit at apogee where:

$$\begin{aligned} r_0 &= 6733.5 \\ \dot{r}_0 &= -1.582e - 11 \\ \theta_0 &= 0 \\ \dot{\theta}_0 &= 0.0011397 \end{aligned} \tag{5.5}$$

The simulation was run for 5 orbits as shown in Figure 4. Figure 5 displays the simulation for 5 periods with eccentricity of 0.005 and nonlinear gravitational terms. For the large relative distance considered, the effect of nonlinearities is significant. The drift for the first few orbits is approximately 1.4 km per orbit. The $J2$ perturbation with an eccentricity of $e = 0.005$ but neglecting the nonlinear gravitational terms, were run for 20 orbits. The initial conditions of the reference orbit given by the STK nonlinear propagator

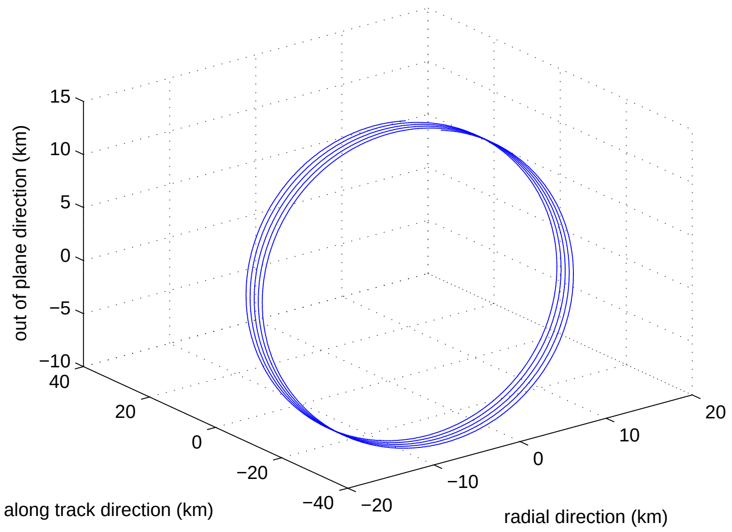

Figure 4: Eccentric orbit using CW initial conditions - 5 orbits with a drift of approximately 1km per orbit

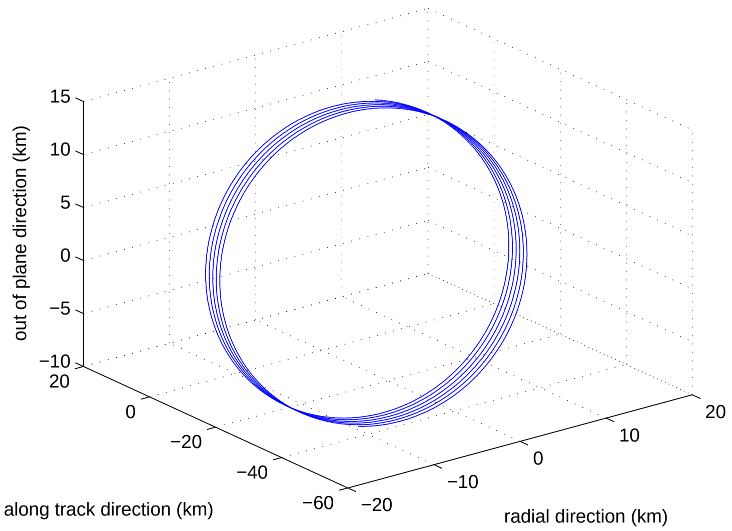

Figure 5: Eccentricity and nonlinear gravitational terms using the CW initial conditions - 5 orbits. The initial drift is approximately 1.4 km per orbit.

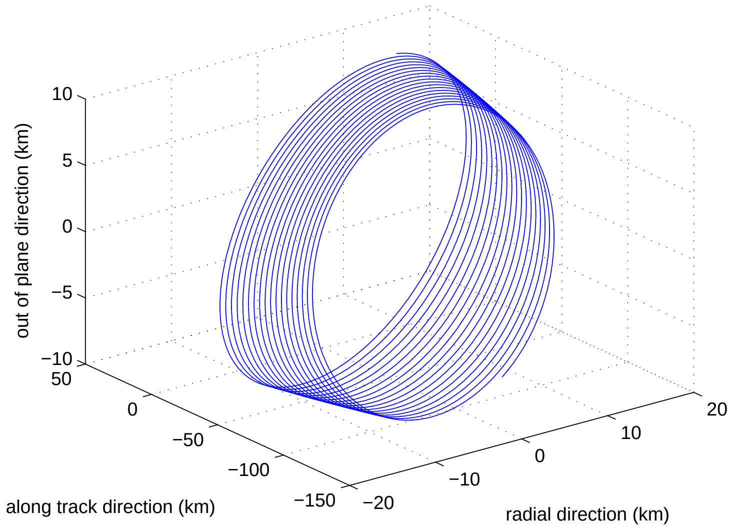

Figure 6: Case with eccentricity and the J_2 perturbation using the CW initial conditions - drift is approximately 3 km per orbit

were:

$$\begin{aligned} r_0 &= 6733.5 \\ \dot{r}_0 &= -2.8383 \times 10^{-5} \\ \theta_0 &= 0 \\ \dot{\theta}_0 &= 0.0011398 \end{aligned} \tag{5.6}$$

Finally, all of the perturbations in the 'study model' were considered, the plot is shown in Figure 7.

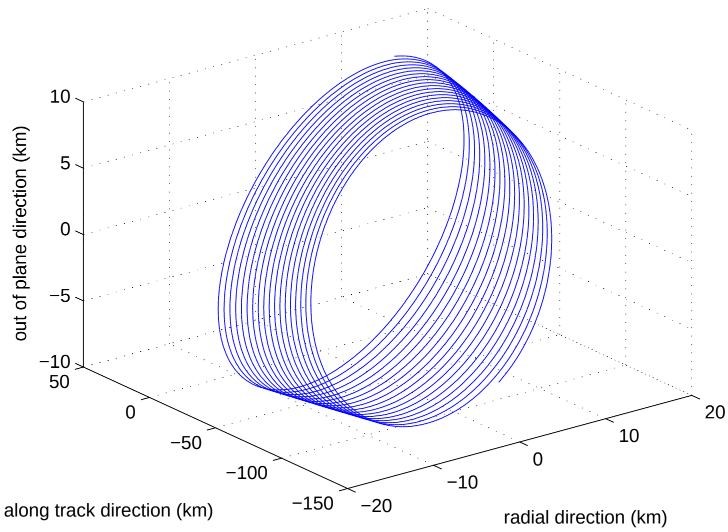

Figure 7: The study model with eccentricity, nonlinear gravitational terms and J_2, using the CW initial conditions where the drift is approximately 3.3 km per orbit.

6 Numerical method for locating periodic or quasi-periodic orbits

In the Hamiltonian formulation of the CW equations, there are explicit initial conditions that give periodic relative motion. As perturbations are added, the same initial conditions will no longer yield closed orbits. However, a numerical method proposed by Marcinek and Pollak [9], based on a variant of Newton's method, may locate stable or unstable periodic orbits. Newton method's has previously been applied to two degrees of freedom continuous systems in [12], where it has been shown that for such systems one may locate all periodic orbits using this method. However, the relative satellite motion model has three degrees of freedom and the increased dimensionality makes the search more complex. Nevertheless, one advantage of the Hamiltonian formulation for relative satellite motion is that a good initial guess for Newton's method is already given for the linear Hamiltonian. This provides a good initial guess and as complexity is added, new initial conditions will be obtained in a stepwise manner.

Here the variant of Newton's method is presented for a three degree of freedom model. The purpose of this method is to find a periodic orbit which has period T^*, i.e. it satisfies the condition

$$\mathrm{X}^*(T^*) = \mathrm{X}^*(0), \tag{6.1}$$

where $\mathrm{X} = [x, p_x, y, p_y, z, p_z]^T$ describes a point in the phase space. The "$*$" notation is used to signify points on the periodic orbit. Newton's method starts at a point $\mathrm{X}(t)$ initiated at $t = 0$ on a surface of section, e.g. $y = 100$ km, and the trajectory returns to the surface of section at some later time T. An assumption of this method is that the initial trajectory is close to the periodic orbit $\mathrm{X}^*(t)$. This means that the trajectory almost closes in upon itself at time T, which is itself approximately T^*. For example, using the initial conditions for periodic solutions in the linear Hamiltonian and then adding the higher order terms of the gravitational potential, will initialize a trajectory close to a periodic orbit.

6.1 Monodromy matrix variant of Newton's method

As the approximate orbit is close to the assumed periodic orbit, the seperation between the two can be calculated using the equations of motion linearized about the approximate orbit $\mathrm{X}(t)$ [12]. This is the analog of using the derivative of the function at a point close to its zero in Newton's Method. Let $\delta\mathrm{X}(t)$ denote a small deviation about the approximate orbit. The linearized equations of motion for this deviation are

$$\delta\dot{\mathrm{X}}(t) = H^{''}(t)\delta\mathrm{X}(t), \tag{6.2}$$

where $H^{''}_{ij}(t) = \partial^2 H/\partial X_j \partial X_i$ is the 6×6 Hessian matrix of the Hamiltonian with respect to the coordinates and momenta evaluated along the approximate trajectory, also called the force constant matrix. The 6×6 monodromy matrix $\mathbf{M}(t)$ is then defined such that

$$\delta\mathrm{X}(t) = \mathbf{M}(t)\delta\mathrm{X}(0) \tag{6.3}$$

and $\mathbf{M}(0) = I$, the unit matrix. The approximate monodromy matrix $\mathbf{M}$ is defined as $\mathbf{M} \equiv \mathbf{M}(T)$. Therefore, the monodromy matrix is defined as

$$\mathbf{M} = \mathrm{e}^{H''(T)T} \tag{6.4}$$

Then the central equation of Newton's method is given as:

$$\mathrm{X}^*(T) - \mathrm{X}(T) \simeq \mathrm{X}^*(0) - \mathrm{X}(T) \simeq \mathbf{M}[\mathrm{X}^*(0) - \mathrm{X}(0)] \tag{6.5}$$

rearranging gives

$$X(T) - X(0) = (I - \mathbf{M})[X^*(0) - X(0)] \tag{6.6}$$

This result gives an iterative improvement to the choice of initial conditions for the periodic orbit

$$X^*(0) = X(0) + (I - \mathbf{M})^{-1}[X(T) - X(0)] \tag{6.7}$$

In practice, one encounters a problem when applying the method to conservative systems, because for any trajectory there are always two directions in phase space which are marginally stable. One is along the trajectory and the other is perpendicular to the energy surface of the orbit. This implies that the $(I - \mathbf{M})$ matrix is singular. For the purposes of this work the singular matrix can be inverted using the Moore-Penrose pseudo-inverse (**pinv** command in Matlab). Alternative methods can be used, such as the manipulations described in [9], however, using the pseudo-inverse works effectively in this case.

6.2 Energy conservation constraint

The method described so far was implemented for the model with eccentricity, for which it did find closed periodic orbits. However, as the orbits are weakly unstable, the search would continue unbounded and new initial conditions found in the search would be extremely large. For this reason it is necessary to include a bound on the numerical search. Because this is a Hamiltonian system, there is a natural bound described by the Hamiltonian function.

An improved guess for the periodic orbit vector $X^*(0)$ uses the additional constraint of energy conservation $\delta H = 0$.

$$\delta H = \frac{\partial H}{\partial x}\delta x + \frac{\partial H}{\partial p_x}\delta p_x + \frac{\partial H}{\partial y}\delta y + \frac{\partial H}{\partial p_y}\delta p_y + \frac{\partial H}{\partial z}\delta z + \frac{\partial H}{\partial p_z}\delta p_z = 0 \tag{6.8}$$

evaluated at time T. Therefore,

$$\left(\frac{\partial H}{\partial x}, \frac{\partial H}{\partial p_x}, \frac{\partial H}{\partial y}, \frac{\partial H}{\partial p_y}, \frac{\partial H}{\partial z}, \frac{\partial H}{\partial p_z}\right) . (\delta x, \delta p_x, \delta y, \delta p_y, \delta z, \delta p_z) = 0 \tag{6.9}$$

The left hand vector from (6.9) can replace a row in the $(I - \mathbf{M})$ matrix and the corresponding row of the vector $(X(T) - X(0))$ is set to zero.

7 Search for periodic or quasi-periodic solutions

In the following subsections, the variant of Newton's method described in Section 4 was applied to locate periodic or quasi-periodic relative satellite motion.

7.1 Eccentricity

Newton's method is successful in finding initial conditions that give near closed periodic solutions for the linear Hamiltonian with eccentricity, where the reference orbit is initialized at

$$\begin{aligned} r_0 &= 6733.5 \\ \dot{r}_0 &= -1.582 \times 10^{-11} \\ \theta_0 &= 0 \\ \dot{\theta}_0 &= 0.0011397 \end{aligned} \tag{7.1}$$

This initializes the reference orbit at apogee with an eccentricity of $e = 0.005$, the semi-major axis $a = 6700km$. The following initial conditions give a near closed orbit, initial drift is approximately 0.001km per orbit. Figure 8

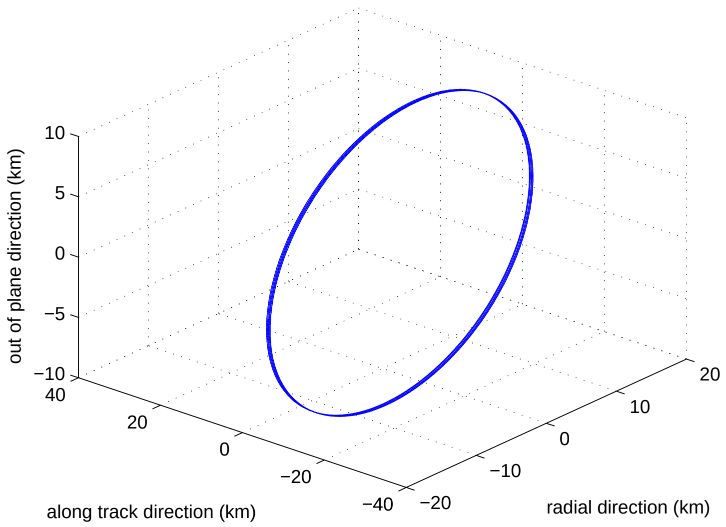

Figure 8: Eccentric orbit corrected - periodic orbit drift is reduced to 0.000983 km per orbit

illustrates this orbit with drift of approximately 0.001km per orbit.

$$
\begin{aligned}
x_0 &= 12.2255 \\
y_0 &= -3.4640 \\
z_0 &= 9.9987 \\
p_{x_0} &= 0.0041 \\
p_{y_0} &= 7.6602 \\
p_{z_0} &= 0
\end{aligned}
\tag{7.2}
$$

Using the canonical transformations

$$
\begin{aligned}
\dot{x}_0 &= p_{x_0} + \dot{\theta}_0 y_0 - \dot{r}_0 \\
\dot{y}_0 &= p_{y_0} - \dot{\theta}_0 (r_0 + x_0) \\
\dot{z}_0 &= p_{z_0}
\end{aligned}
\tag{7.3}
$$

the initial conditions in cartesian coordinates are calculated as:

$$
\begin{aligned}
x_0 &= 12.2255 \\
y_0 &= -3.4640 \\
z_0 &= 9.9987 \\
p_{x_0} &= -1.58 \times 10^{-4} \\
p_{y_0} &= -0.0279 \\
p_{z_0} &= 0
\end{aligned} \tag{7.4}
$$

7.2 Eccentricity and nonlinear gravitational terms

Newton's method greatly reduces the drift of the trajectory as is shown in Figure 9. Although an exact periodic orbit could not be found the drift is approximately 0.00084 km per orbit, using the following initial conditions:

$$
\begin{aligned}
x_0 &= 12.3306 \\
y_0 &= -4.2202 \\
z_0 &= 9.9989 \\
p_{x_0} &= 0.0049 \\
p_{y_0} &= 7.6601 \\
p_{z_0} &= 0
\end{aligned} \tag{7.5}
$$

and in Cartesian coordinates

$$
\begin{aligned}
x_0 &= 12.3306 \\
y_0 &= -4.2202 \\
z_0 &= 9.9989 \\
\dot{x}_0 &= 9.0238 \times 10^{-5} \\
\dot{y}_0 &= -0.0281 \\
\dot{z}_0 &= 0
\end{aligned} \tag{7.6}
$$

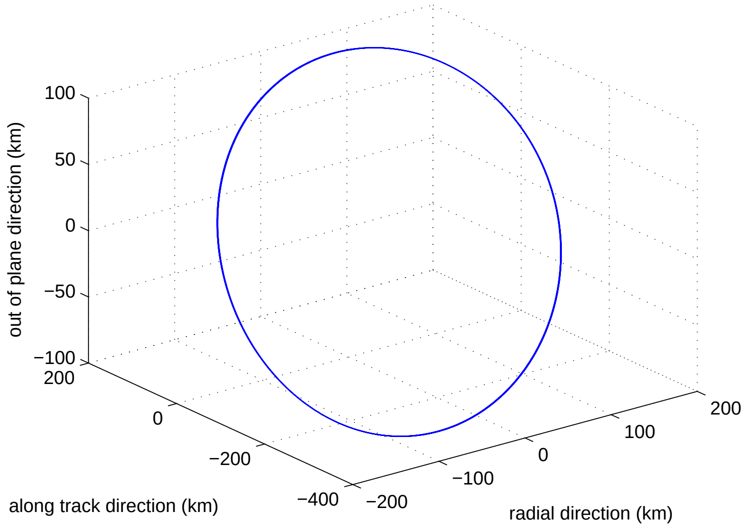

Figure 9: Eccentricity and nonlinear order gravitational terms with corrected initial condition. The initial drift is approximately 0.00084 km per orbit

7.3 J2 perturbation with eccentricity

The initial conditions of the reference orbit given by the STK propagator are:

$$
\begin{aligned}
r_0 &= 6733.5 \\
\dot{r}_0 &= -2.8383 \times 10^{-5} \\
\theta_0 &= 0 \\
\dot{\theta}_0 &= 0.0011398
\end{aligned}
\tag{7.7}
$$

Applying Newton's method finds initial conditions that give a bounded solution as shown in Figure 10, where:

$$\begin{aligned}
x_0 &= 10.1631 \\
y_0 &= 10.0012 \\
z_0 &= 9.9901 \\
p_{x_0} &= 0 \\
p_{y_0} &= 7.663 \\
p_{z_0} &= -0.0003
\end{aligned} \tag{7.8}$$

and in Cartesian coordinates:

$$\begin{aligned}
x_0 &= 10.1631 \\
y_0 &= 10.0012 \\
z_0 &= 9.9901 \\
\dot{x}_0 &= 0.0114 \\
\dot{y}_0 &= -0.0233 \\
\dot{z}_0 &= -0.0003
\end{aligned} \tag{7.9}$$

No closed periodic orbits could be found with J_2 and eccentricity.

7.4 The study model with eccentricity, nonlinear gravitational terms and the J2 perturbation

Using the initial conditions from (7.7) and applying Newton's method found the initial conditions below that give a bounded, quasi-periodic orbit. Figure 11 shows the relative trajectory for the nonlinear study model, which includes

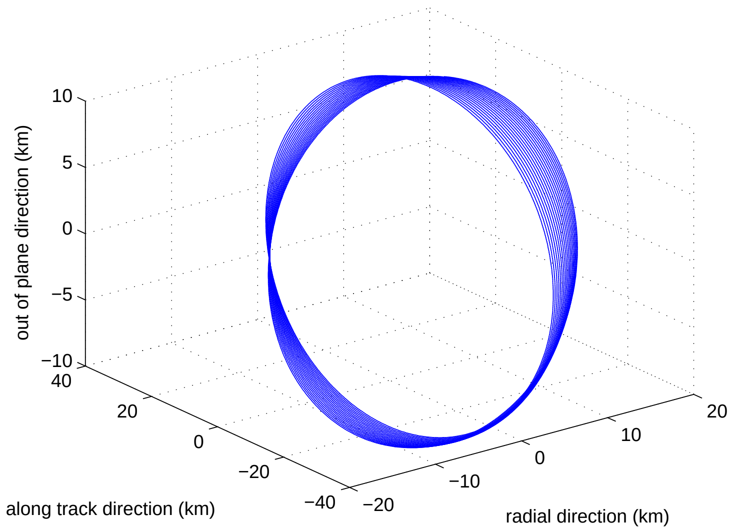

Figure 10: J_2 and eccentricity with corrected initial conditions. The trajectory is bounded.

eccentricity of 0.005, nonlinear gravitational terms and J_2:

$$\begin{aligned} x_0 &= 9.6556 \\ y_0 &= 10.0036 \\ z_0 &= 9.9681 \\ p_{x_0} &= 0 \\ p_{y_0} &= 7.6636 \\ p_{z_0} &= -0.0012 \end{aligned} \tag{7.10}$$

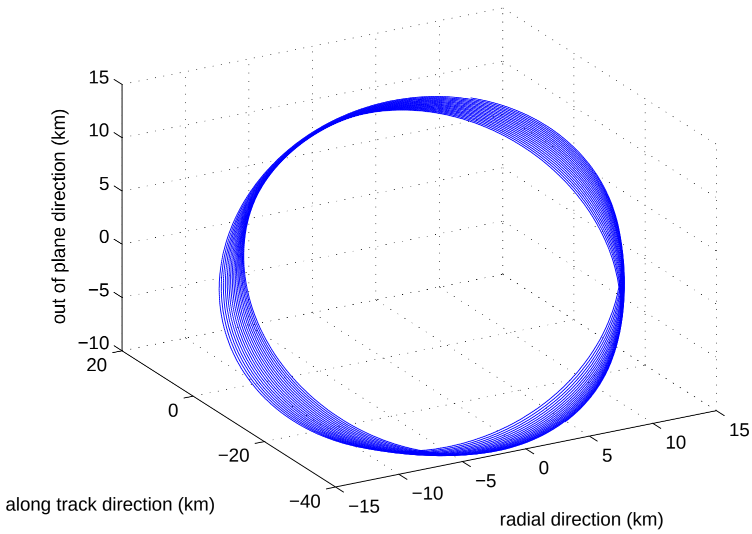

Figure 11: The nonlinear study model with eccentricity, nonlinear gravitational terms and J_2 - the trajectory is bounded.

and in cartesian coordinates

$$
\begin{aligned}
x_0 &= 9.6556 \\
y_0 &= 10.0036 \\
z_0 &= 9.9681 \\
\dot{x}_0 &= 0.0114 \\
\dot{y}_0 &= -0.0221 \\
\dot{z}_0 &= -0.0012
\end{aligned}
\tag{7.11}
$$

It is desirable to evaluate the performance of Newton's method with wider formations. The wider simulation was set at $[x_0, y_0, z_0] = [50km, 50km, 50km]$ as the initial condition in Newton's method. The Newton method successfully located a bounded trajectory (20 orbit), with the following initial conditions:

$$\begin{aligned}
x_0 &= 49.04\\
y_0 &= 50.01\\
z_0 &= 49.8072\\
p_{x_0} &= 0\\
p_{y_0} &= 7.6181\\
p_{z_0} &= -0.0073
\end{aligned} \tag{7.12}$$

and in cartesian coordinates:

$$\begin{aligned}
x_0 &= 49.04\\
y_0 &= 50.01\\
z_0 &= 49.8072\\
\dot{x}_0 &= 0.0570\\
\dot{y}_0 &= -0.1125\\
\dot{z}_0 &= -0.0073
\end{aligned} \tag{7.13}$$

which gave the trajectory for 20 orbits shown in Figure 12.

8 Principal Component Analysis

Bounded or slowly drifting trajectories found using Newton's method, are not necessarily periodic. Using these trajectories as a reference in a real system would involve a real time simulation of the relative motion. The control methodology requires that for practical implementation, the reference trajectory be periodic. A statistical technique known as principle component analysis (PCA) was used to project the bounded or slowly drifting trajectories onto planar and almost closed periodic orbits. Once fitted using sinusoidal

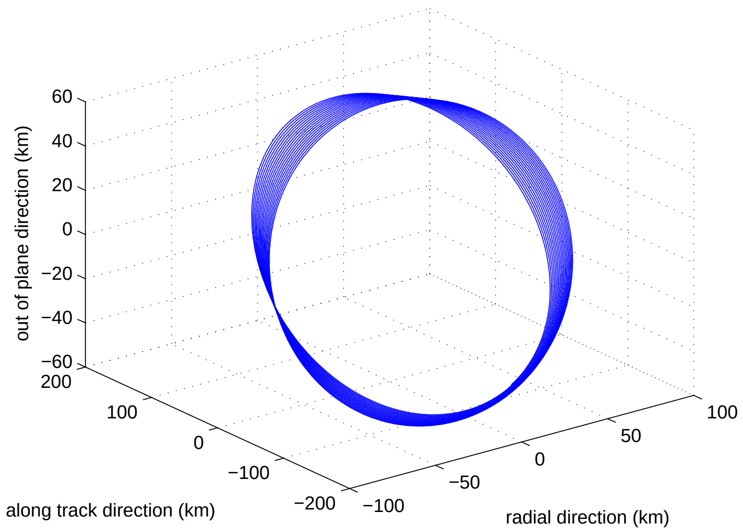

Figure 12: Nonlinear study model with eccentricity, nonlinear gravitational terms and J_2 for approximately 100km mean separation - the trajectory appears bounded for 20 orbits.

functions, as described below in this report, the trajectories are suitable to be used as reference trajectories for control purposes.

PCA is a powerful tool (see [20]) for analyzing data and has found application in fields such as face recognition and image compression, and is a common technique for finding patterns in data of high dimension. PCA rotates the coordinate system such that the maximum variability is aligned along the axis of the new system. The first principal component accounts for as much of the variability in the data as possible, and in the direction orthogonal to the subspace spanned by the former components. The bounded trajectory (20 orbits) data is used to obtain the principle components, the principal components are then used to rotate the first period of the trajectory. Figure 13 shows this projected trajectory together with the original bounded trajectory, illustrated for the 'study model' with initial conditions (7.10).

PCA was used to obtain a data set for the reference trajectory, however it is also necessary to project the corresponding canonical momenta, as the method used for closed-loop control requires full state feedback. As the data set gives position and time it is simple to calculate the velocity components using Matlab and therefore using the canonical transformation (7.3) calculate the projected canonical momenta. The method of PCA is a useful tool to determine practical reference trajectories for control implementation.

9 The full model

In this project, a set of *study models* with increasing complexity have been used to find periodic or quasi-periodic trajectories of relative satellite motion, which in turn can be used to determine a reference trajectory for closed-loop control simulations. A further model, known in this project as the *full*

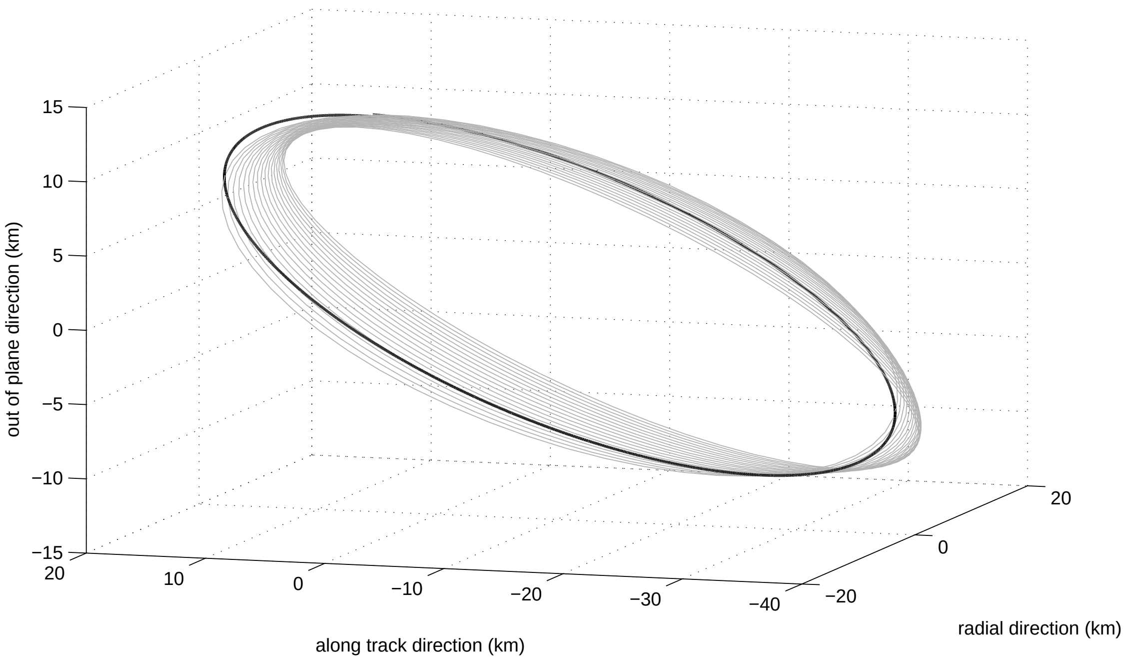

Figure 13: Projected Reference Trajectory - grey trajectory illustrates the bounded solution used to obtain the Principle Components the black trajectory illustrates the projected trajectory.

model, is used to simulate the relative motion under closed loop control. The full model includes higher order gravitational terms, zonal harmonics, eccentricity, and actuation variables to manipulate the relative motion to follow the reference trajectory.

The action of satellite thrusters can be modelled as impulsive changes to the satellites' velocities. In [17] the control inputs are chosen to be the impulsive velocity increments $[\Delta\dot{x}, \Delta\dot{y}, \Delta\dot{z}]$. In the Hamiltonian formulation the control actuators are implemented as impulsive canonical momenta increments $[u_x,\, u_y, u_z] = [\Delta p_x, \Delta p_y, \Delta p_z]$. Given the canonical transformation (7.3) it is easy to see that impulsive canonical momenta increments are equivalent to impulsive velocity increments. The equations of motion for the full model are given in Appendix C.

10 Closed Loop Control

In order to evaluate the effect of the quality of the model used to generate the periodic reference trajectory, a study involving closed loop control of a simulated master/follower formation was performed.

10.1 Linearization of the relative motion dynamics

The nonlinear relative motion dynamics with actuation can be written as follows:

$$\dot{X}(t) = f(X(t)) + \bar{B}u(t) \tag{10.1}$$

where $X = [x,\ y,\ z,\ p_x,\ p_y,\ p_z]^T$ is the state vector consisting of relative positions and canonical momenta, and $u = [u_x,\ u_y,\ u_z]^T$ is a vector of actuations (in units of acceleration), $f(X)$ is a smooth vector field, and $\bar{B}$ is given by:

$$\bar{B} = \begin{bmatrix} 0 & 0 & 0 \\ 0 & 0 & 0 \\ 0 & 0 & 0 \\ 1 & 0 & 0 \\ 0 & 1 & 0 \\ 0 & 0 & 1 \end{bmatrix} \tag{10.2}$$

It is assumed that the relative motion is controlled by adjusting the motion of the follower satellite only.

Define a reference trajectory $X_r(t) \in \Re^6$ over a time interval $t \in [t_0, t_f]$, which approximately satisfies

$$\dot{X}_r(t) \approx f(X_r(t)) \tag{10.3}$$

Notice that it is reasonable to make this approximation as the reference trajectory to be used approximates a solution of the relative motion dynamics given by (10.1) with $u = 0$.

Consider small deviations $x(t)$ from $X_r(t)$, such that $x(t) = X(t) - X_r(t)$. Then the perturbed dynamics with actuation are given by:

$$\dot{X}(t) = \dot{X}_r(t) + \dot{x}(t) = f(X_r(t) + x(t)) + \bar{B}u \tag{10.4}$$

Using a Taylor series expansion about $X_r(t)$ and neglecting terms of order higher than one, gives:

$$\dot{X}_r(t) + \dot{x}(t) \approx f(X_r(t)) + \left[\frac{\partial f}{\partial x}\right]\bigg|_{X_r(t)} x(t) + \bar{B}u \tag{10.5}$$

But since $\dot{X}_r(t) \approx f(X_r(t))$, it is possible to write the following expression for the deviations from the reference:

$$\dot{x}(t) \approx \bar{A}(t)x(t) + \bar{B}u(t) \tag{10.6}$$

where

$$\bar{A}(t) = \left[\frac{\partial F}{\partial x}\right]\bigg|_{X_r(t)} \tag{10.7}$$

To simplify the control design, it is assumed that $\bar{A}(t)$ does not change much along the reference trajectory so that, for the purposes of control design, the following time invariant model is assumed:

$$\dot{x} = \bar{A}x(t) + \bar{B}u(t) \tag{10.8}$$

where

$$\bar{A} = \left[\frac{\partial F}{\partial x}\right]\bigg|_{X_0} \tag{10.9}$$

and X_0 is a suitable point that belongs to the reference trajectory $X_r(t)$. For the purposes of this study, X_0 was defined as the initial point of the trajectory $X_r(t_0)$. It should be noted that in this application tighter control should be possible by considering the changes in $\bar{A}(t)$ along the reference trajectory.

10.2 Model discretisation

Consider that the actuation is performed using thrusters which provide impulsive thrust with a sampling interval T_s and a duration d, such that it is reasonable to assume that the control vector u is defined as follows:

$$u(t) = \begin{cases} u_k/d & t_k \leq t \leq t_k + d \\ 0 & t_k + d < t < t_k + T_s \end{cases} \tag{10.10}$$

where k is a sampling index, t_k is a sampling instant, such that $t_k = kT_s$, and $u_k = [\Delta v_x,\, \Delta v_y,\, \Delta v_z]^T$ is the control signal (in velocity units) provided by a discrete-time controller. The magnitude $||u_k|| = \sqrt{\Delta v_x^2 + \Delta v_y^2 + \Delta v_z^2}$ will also be known as DeltaV in this report, while the sum:

$$\sum_{k=0}^{k} ||u_k|| \tag{10.11}$$

will be called accumulated DeltaV.

In the limit case when $d \to 0$ and $T_s > d$, a control signal defined by (10.10) becomes impulsive control of the form:

$$u(t) = u_k \delta(t - t_k),\ t_k \leq t < t_{k+1},\ k = 0, 1, 2, \ldots \tag{10.12}$$

where $\delta(t - t_k)$ is the Dirac delta function, defined by:

$$\delta(t - t_k) = 0, t \neq t_k \tag{10.13}$$

and

$$\int_{-\infty}^{\infty} \delta(\tau) d\tau = 1 \tag{10.14}$$

In the case where the sampling period is the same as the pulse duration $T_s = d$, then the control signal is $u(t) = u_k/d$ for $t_k \leq t \leq t_{k+1}$, such that the control signal is constant between sampling instants, which is a common assumption in discrete-time control.

To discretise the linear time invariant model (10.8), the state at the next sampling instant $x_{k+1} = x(t_{k+1}) = x(t_k + T_s)$ is found given the state at the current sampling instant $x_k = x(t_k)$ and the control action during the sampling interval $t \in [t, t + T_s]$ (see [18]):

$$x(t_{k+1}) = e^{\bar{A}T_s} x(t_k) + \int_{t_k}^{t_{k+1}} e^{\bar{A}(t_{k+1}-\tau)} \bar{B} u(\tau) d\tau \tag{10.15}$$

But since $u(t) = u_k/d$ for $t_k \leq t \leq t_k + d$ and $u(t) = 0$ for $t_k + d \leq t \leq t_{k+1}$, then

$$x(t_{k+1}) = e^{\bar{A}T_s} x(t_k) + \int_{t_k}^{t_k+d} e^{\bar{A}(t_{k+1}-\tau)} d\tau \bar{B} u_k/d \tag{10.16}$$

Using the change of variables $\tau = r + t_k$

$$\begin{aligned} x(t_{k+1}) &= e^{\bar{A}T_s} x(t_k) + \int_0^d e^{\bar{A}(t_{k+1}-t_k-r)} dr \bar{B} u_k/d \\ x(t_{k+1}) &= e^{\bar{A}T_s} x(t_k) + \int_0^d e^{\bar{A}(T_s-r)} dr \bar{B} u_k/d \\ x(t_{k+1}) &= e^{\bar{A}T_s} x(t_k) + e^{\bar{A}T_s} \int_0^d e^{-\bar{A}r} dr \bar{B} u_k/d \end{aligned} \tag{10.17}$$

So that the discrete time model can be expressed as follows:

$$x_{k+1} = Ax_k + Bu_k \tag{10.18}$$

where

$$\begin{aligned} A &= e^{\bar{A}T_s} \\ B &= e^{\bar{A}T_s} \int_0^d e^{-\bar{A}r} dr \bar{B}/d \end{aligned} \tag{10.19}$$

10.3 Discrete Linear Quadratic Regulator with impulsive actuation

The control technique employed was the discrete linear quadratic regulator (LQR) [19] with impulsive actuation. The LQR technique was chosen due to its ability to handle the problem of formation flying control, as has already been shown in the literature [17], and also due to its simplicity for practical implementation purposes. Impulsive control was chosen to approximate the way actual satellite thrusters work.

Suppose that in order to track a reference trajectory, the following quadratic performance index is minimised:

$$J = \tfrac{1}{2} \sum_{k=0}^{\infty} \left[x_k^T Q x_k + u_k^T R u_k \right] \tag{10.20}$$

Assume that Q is a positive semidefinite matrix and that R is positive definite. It is also assumed that the pair (A, B) is stabilisable and that the pair $(A, \sqrt{Q})$ is observable [19].

The minimisation of (10.20) subject to the linear discrete-time dynamics (10.18) can be achieved by the well know Ricatti solution [19]. First, find the solution of the following algebraic Ricatti equation:

$$S = A^T \left[S - SB(B^T SB + R)^{-1} B^T S \right] A + Q \tag{10.21}$$

The state feedback gain is given by:

$$K = \left(B^T SB + R \right)^{-1} B^T SA \tag{10.22}$$

Notice that, given values of A, B, Q and R, matrices S and K can be computed off-line (using for example the dlqr command in Matlab), so that the optimal control law is a simple state feedback given by:

$$u_k = -Kx_k \tag{10.23}$$

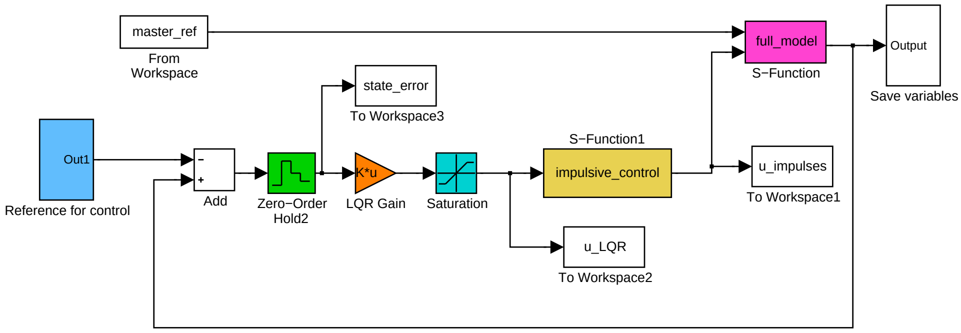

Figure 14: Simulink diagram of the closed loop simulation of relative satellite motion.

In term of the original states $X(t)$ and the reference trajectory $X_r(t)$, the control law is given by:

$$u_k = -K(X(t_k) - X_r(t_k)) \tag{10.24}$$

10.4 Results

Relative satellite motion has been simulated in closed loop using the impulsive LQR controller described above. The 'full model' used to simulate the dynamics of the system is similar to the most complex 'study model', including gravitational nonlinearities, eccentricity and J2 perturbations, and in addition including the actuation. The simulations were performed in the Matlab/Simulink environment. Figure 14 shows the Simulink system employed for the closed-loop simulations.

In order to implement the reference trajectories for control as functions of time in non-trivial cases, each state variable trajectory projected by PCA was fitted to a sinusoidal function of time of the form:

$$r_i(t) = a_i \sin(\omega_i t + \phi_i) + b_i, i = 1, \ldots, 6 \tag{10.25}$$

Table 1: Cases under consideration according to the effects considered in the model used to generate the reference trajectory for control, the model used to generate the controller, the sampling period of the controller, and the control weighing matrix.

Case	**Ref. Traj.**	**Controller**	**Sampling (s)**	R
1	HCW	HCW	4	$10^3 I_{[3\times3]}$
2	e	e	4	$10^5 I_{[3\times3]}$
3	e+NL	e+NL	4	$10^5 I_{[3\times3]}$
4	e+J2	e+J2	4	$10^9 I_{[3\times3]}$
5	e+NL+J2	e+NL+J2	4	$10^9 I_{[3\times3]}$
6	e+NL+J2	e+NL+J2	60	$10^9 I_{[3\times3]}$
7	e+NL+J2	e+NL+J2	1	$10^9 I_{[3\times3]}$
8	e+NL	e+NL+J2	4	$10^9 I_{[3\times3]}$
9	e+NL+J2	e+NL	4	$10^9 I_{[3\times3]}$
10	e+NL+J2 (not projected)	e+NL+J2	4	$10^9 I_{[3\times3]}$

Key: HCW= Hill–Clohessy–Wiltshire model, e= eccentricity, NL= gravitational nonlinearities, J2= zonal harmonic effect

This simple function structure provided a good fit, with appropriate values for the parameters $(a_i, \omega_i, \phi_i, b_i)$, in all cases considered.

The cases considered are summarised in Table 1. In all cases, except from case 1, the eccentricity value considered was $e = 0.005$. In all cases the duration of the thrust pulses was $d = 1$ s. The state weighing matrix was chosen as $Q = I_{[6\times6]}$, while the values of the control weighing matrix are given in Table 1.

Figures 15 to 30 show the simulation results for all cases. Table 2 shows

Table 2: Accumulated DeltaV requirement per orbit, and maximum tracking error

Case	DeltaV per orbit (km/s)	Max. tracking error (km)
1	0.015171	1.0190
2	0.015758	1.1475
3	0.015707	1.1603
4	0.0079409	1.0019
5	0.00599	1.2710
6	0.0081389	5.3957
7	0.0095239	0.7155
8	0.065304	10.6493
9	0.011417	0.8046
10	0.00037039	0.0455

for each case the required total DeltaV per orbit of relative motion, as well as the maximum tracking error magnitude.

10.5 Analysis of Control Results

From Table 2, comparing the results of cases 1 to 5, it can clearly be seen how the use of a model including the J2 perturbation as well as eccentricity and nonlinearities provided the least DeltaV value per orbit, for a similar tracking error performance. The reduction in the DeltaV value achieved in case 5 compared with cases 1 to 3 is about 61%, while the reduction in DeltaV value achieved in case 5 compared with case 4 is about 24%.

Comparing cases 5, 6 and 7, it can be seen that increasing the sampling time from 4 s to 60 s significantly increased the tracking error and also increased the DeltaV per orbit, while reducing the sampling time from 4 s to 1 s reduced the tracking error by 43 % but increased the DeltaV value per orbit by 35.9 %.

Comparing cases 8 and 5, it can be observed that using a reference trajectory of a less detailed model (with eccentricity and nonlinearities but without the J2 effect) with a controller generated from a model that included the J2 effect, resulted in a significant increase in the tracking error, together with an increase in the DeltaV requirement per orbit.

Comparing cases 9 and 5, it can be seen that using a controller obtained from a less detailed model (with eccentricity and nonlinearities but without the J2 effect) and a reference trajectory generated from a model that included the J2 effect, resulted in an increase of the DeltaV value of about 99%, while the tracking error decreased by about 36%.

Case 10 used a non–projected reference trajectory, as simulated by the 'study model' with a fixed step size 4th order Runge Kutta integrator with a step size of 1 s, while the closed loop system was simulated with a variable step size Runge-Kutta integrator. Given that in this work the 'study model' and the 'full model' consider the same effects, the fact that some very small control action was required is explained by the difference in the integrator used. It should be noted, however, that this kind of reference trajectory would not be very practical as it is not periodic, unless it is intended to be used for short periods. It would be ideal if extra effects such as air drag were considered in the 'full model'. However, extra effects could not be implemented in this project due to time constraints.

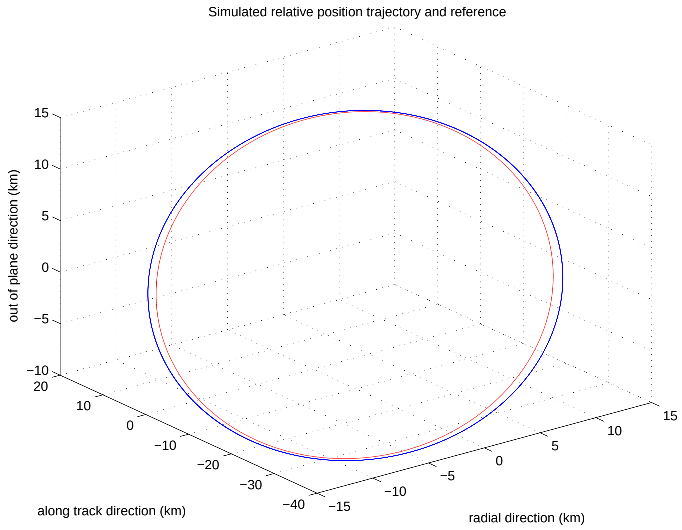

Figure 15: Case 1: Reference and controller from HCW equations. Relative position trajectory

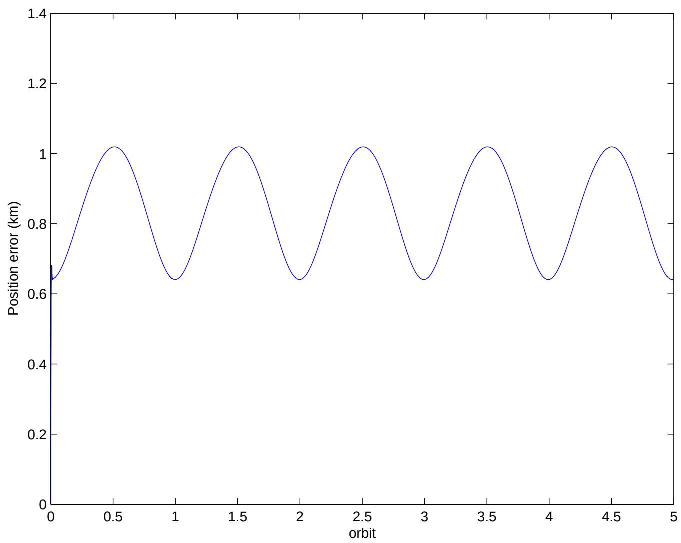

Figure 16: Case 1: Reference and controller from HCW equations. Position error

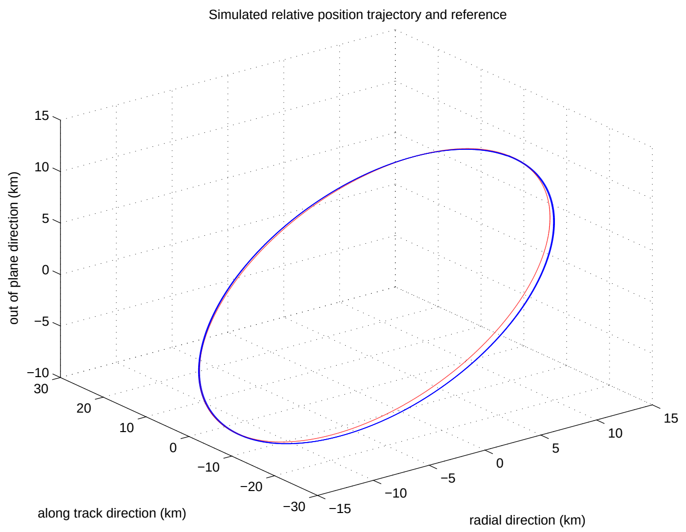

Figure 17: Case 2: Reference and controller from model including eccentricity. Relative position trajectory

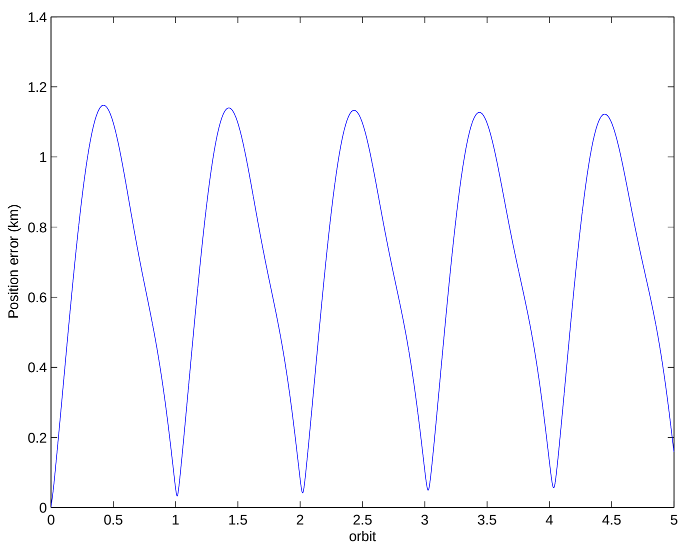

Figure 18: Case 2: Reference and controller from model including eccentricity. Magnitude of tracking error

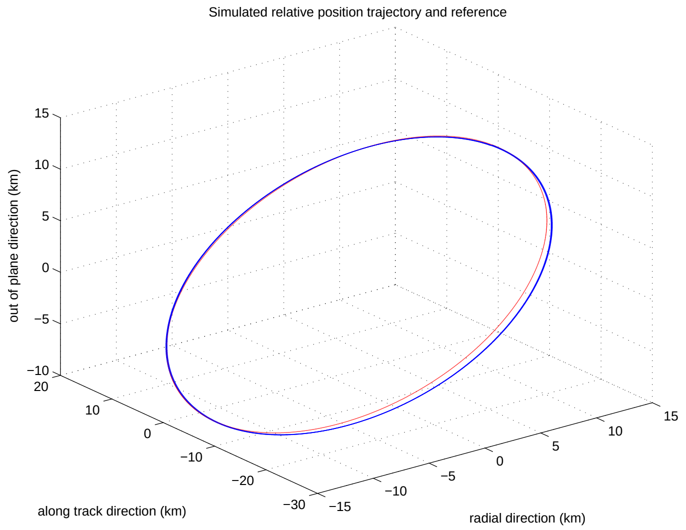

Figure 19: Case 3: Reference and controller from model including eccentricity and nonlinearities. Relative position trajectory

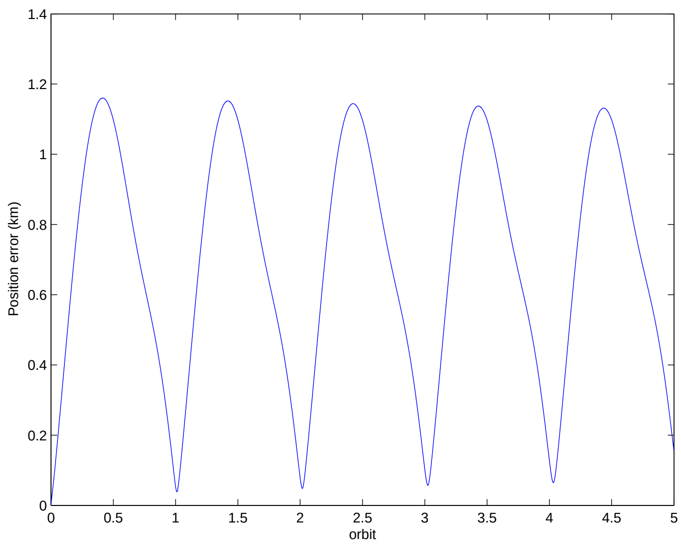

Figure 20: Case 3: Reference and controller from model including eccentricity and nonlinearities. Magnitude of tracking error

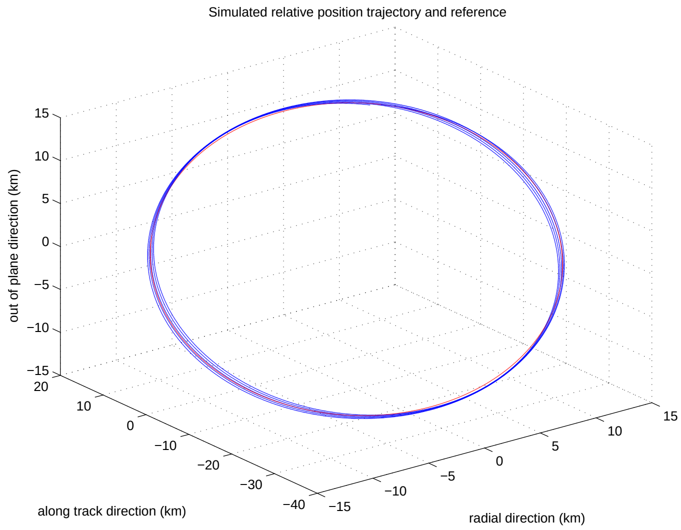

Figure 21: Case 4: Reference and controller from model including eccentricity and J2. Relative position trajectory

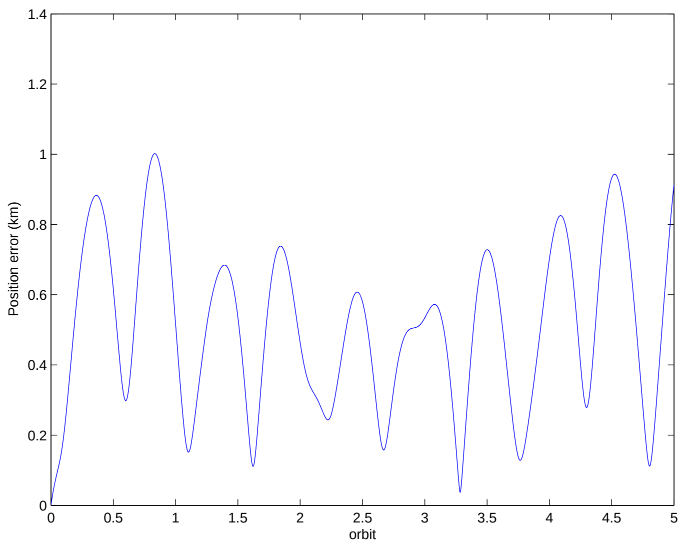

Figure 22: Case 3: Reference and controller from model including eccentricity and J2. Magnitude of tracking error

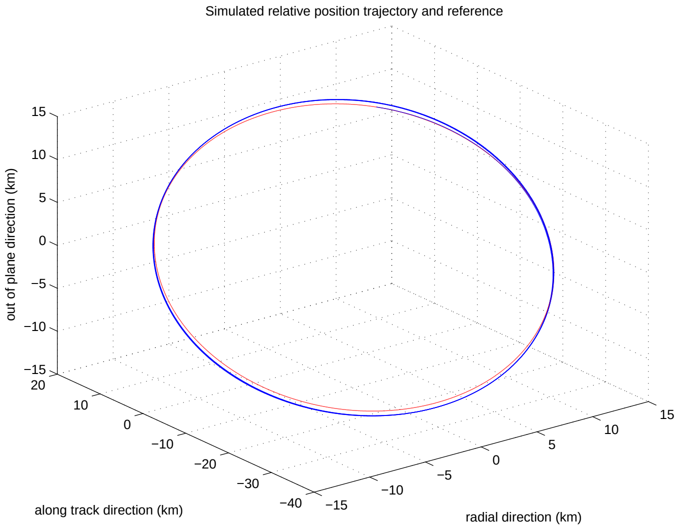

Figure 23: Case 5: Reference and controller from model including eccentricity, nonlinearities and J2. Relative position trajectory

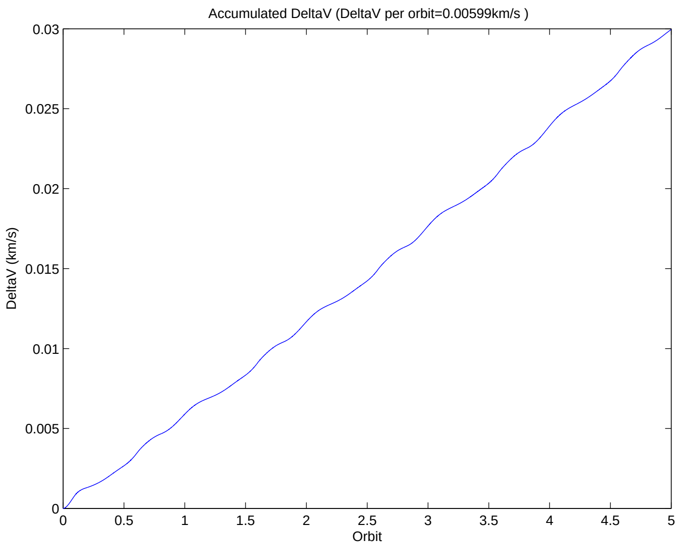

Figure 24: Case 5: Reference and controller from model including eccentricity, nonlinearities and J2. Accumulated DeltaV

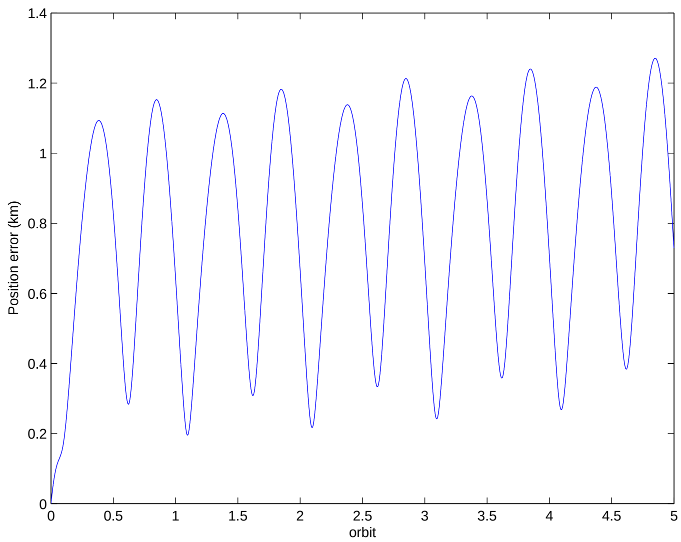

Figure 25: Case 5: Reference and controller from model including eccentricity, nonlinearities and J2. Magnitude of tracking error

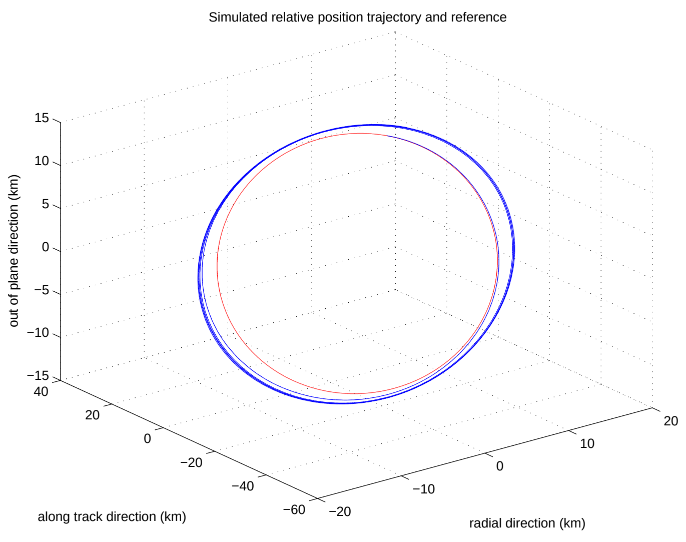

Figure 26: Case 6: Reference and controller from model including eccentricity, nonlinearities and J2, sampling time 60 s. Relative position trajectory

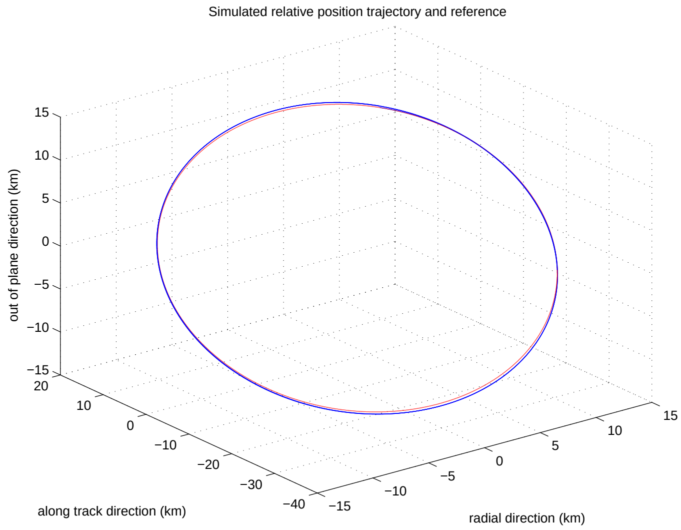

Figure 27: Case 7: Reference and controller from model including eccentricity, nonlinearities and J2, sampling time 1 s. Relative position trajectory

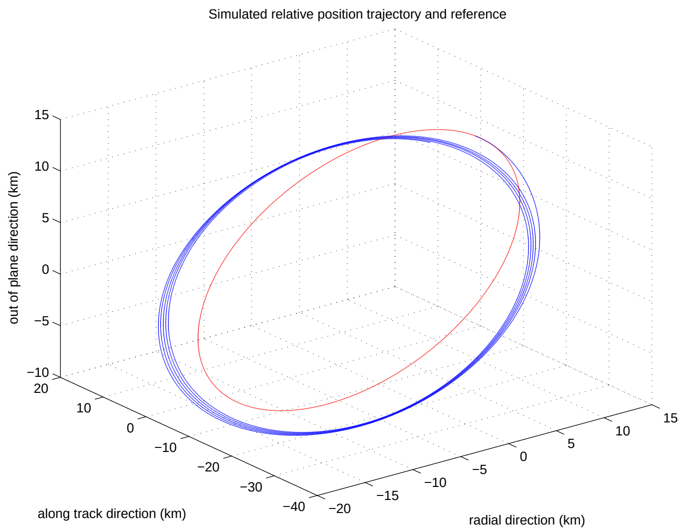

Figure 28: Case 8: Reference from a model including eccentricity and nonlinearities, controller from model including eccentricity, nonlinearities and J2. Relative position trajectory

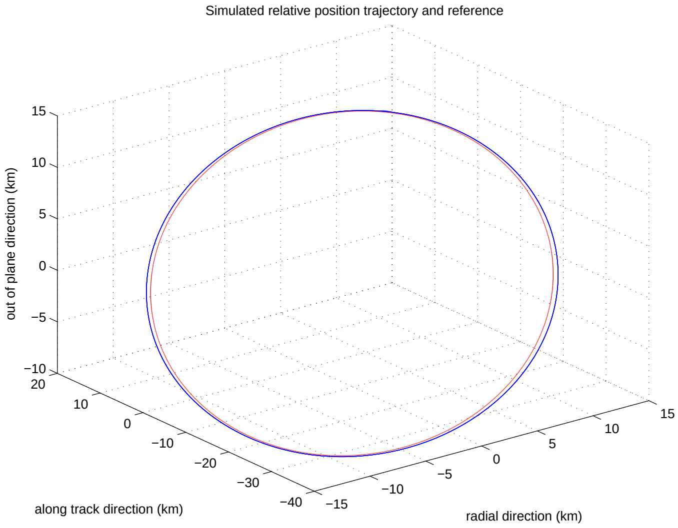

Figure 29: Case 9: Reference from a model including eccentricity and nonlinearities and J2, controller from model including eccentricity, nonlinearities, but not J2. Relative position trajectory

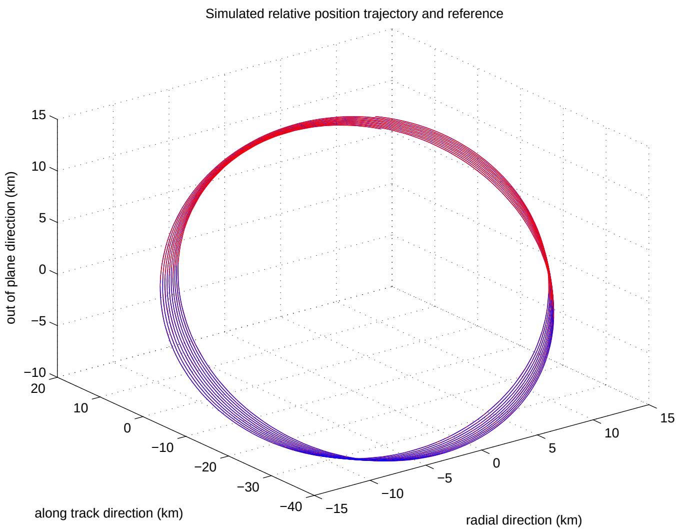

Figure 30: Case 9: Non-projected (natural) reference obtained from a model including eccentricity and nonlinearities and J2, controller from model including eccentricity, nonlinearities and J2. Relative position trajectory

11 Conclusions

In this report a Hamiltonian formulation of relative satellite motion is presented which in its linear form is shown to be equivalent to the well known HCW equations. This formulation is useful as it can be fit into well known linear control theory and explicit solutions can be obtained. The advantage of the Hamiltonian formulation is that perturbations can be added with ease. For the implementation of the numerical method a nonlinear hamiltonian study model is derived which incorporates the eccentricity of the reference orbit, the nonlinear gravitational terms and J_2.
A variant of Newton's method is presented and applied to locate periodic or quasi-periodic relative satellite motion. Advantages of using Newton's method to search for periodic or quasi-periodic relative satellite motion include simplicity of implementation, repeatability of solutions due to its non-random nature, and fast convergence.

The method was able to find near closed periodic orbits in the linear model with eccentricity only. For the nonlinear model with eccentricity, although no closed solutions could be found the drift was greatly reduced. When considering the linear model with J_2, a bounded quasi-periodic solution was found. When nonlinear gravitational terms, eccentricity and J_2 were considered together, the application of the Newton's method located a bounded quasi-periodic solution. These initial conditions found were verified using the well known STK propogator to give bounded solutions.

Given that the use of bounded or drifting trajectories as control references carries practical difficulties over long-term missions, a method based on principal component analysis was developed to project a bounded or slowly drifting trajectory found using Newton's method, to a plane of defined by the first two principal components. In this way a planar trajectory can be produced which is almost closed. The state variables on this projected trajectories can in turn be fitted to sinusoidal functions to provide closed periodic trajectories that preserve useful information about the original bounded or slowly drifting trajectory. These projected and fitted periodic trajectories were used as reference trajectories in closed loop control simulations. The results obtained indicate that the quality of the model employed for generating the reference trajectory used for control purposes has an important influence on the resulting amount of fuel required to track the reference trajectory. The model used to generate LQR controller gains also has an effect on the efficiency of the controller. The sampling time employed is also important, as the shorted the sampling interval, the tighter the control. Finally, as in all control applications, careful consideration must be given to tuning the controller.

12 Future Work

The advantage of the Hamiltonian formulation is that it is easy to add complexity to the model. Therefore, higher order zonal harmonics can be added on to the hamiltonian function. The model incorporates air drag but uses a simplified atmospheric density model. An improvement to the full would be to incorporate a more complex atmospheric model. One avenue for further study would be to investigate the effect of an inclined reference orbit on the type of solutions found using the Newton method.

References

[1] Clohessy, W.H., Wiltshire, R.S., 'Terminal guidance for satellite tendezvous'. Journal of the Aerospace Sciences, 27(9),pp. 653-658, 1960.

[2] Vaddi, S.S., Vadali, S.R., Alfriend, K.T., 'Formation Flying: Accommodating Nonlinearity and Eccentricity Perturbations'. Journal of Guidance, Control, and Dynamics, 26(2), 2003.

[3] Bate, R., Mueller, D., White, J., 'Fundamentals of Astrodynamics'. Dover Publications, New York, 1971.

[4] Inalhan, G., Tillerson, M., How, J., 'Relative Dynamics and Control of Spacecraft Formations in Eccentric Orbits'. Journal of Guidance, Control, and Dynamics, 25(1), 2002.

[5] Mishne, D., 'Formations Control of Satellites Subject to Drag Variations and J_2 Perturbations'. Journal of Guidance, Control, and Dynamics, 27(4), 2004.

[6] Shaub, H. S., and Alfriend, K. T., 'J_2 Invariant Reference Orbits for Spacecraft Formation'. Celestial Mechanics and Dynamical Astronomy, 79(2), 2002, p.77-95.

[7] Wiesel, W. E., 'Relative Satellite Motion About an Oblate Planet'. Journal of Guidance, Control, and Dynamics, 25(4), 2002.

[8] Kasdin, N.J. and Gurfil, P., 'Hamiltonian Modelling of Relative Motion'. Annual New York Academy Science, 1017, 2004, p.138-157.

[9] Marcinek, R.J., and Pollak, E., 'Numerical methods for locating stable periodic orbits embedded in a largely chaotic system'. Journal of Chemical Physics, 100(8), 1994, p.5894-5904.

[10] Kasdin, N.J., and Kolemen, E., 'Bounded, Periodic Relative Motion using Canonical Epicyclic Orbital Elements'. 15th AAS/AIAA Space Flight Mechanics Meeting, Copper Mountain Colorado, 23-27 January 2005.

[11] R.H. Battin, 'An Introduction to the Mathematics and Methods of Astrodynamics', AIAA, 1999.

[12] D. Grobgeld, E. Pollak, J Zakrzewski, 'A numerical method for locating periodic orbits in chaotic systems', Physica D,56, 1992, p368-380.

[13] W.E. Wiesel, 'Spaceflight Dynamics', Irwin/McGraw-Hill, 1997.

[14] D. Izzo. 'Formation flying for MUSTANG'. MSc Dissertation. MSc in Astronautics and Space Engineering, Cranfield University, School of Engineering, 2002.

[15] Wiesel, W. E., 'Relative Satellite Motion About an Oblate Planet'. Journal of Guidance, Control, and Dynamics, 25(4), 2002.

[16] Misjne, D, 'Formation Control of Satellites Subject to Drag Variations and J2 perturbations'. Journal of Guidance, Control, and Dynamics, 27(4), 2004.

[17] A.G. Sparks, 'Satellite Formationkeeping Control in the Presence of gravity perturbations', Proc. American Control Conference, p. 844-848, 2000.

[18] C.T. Chen. 'Linear System Theory and Design'. New York: Oxford University Press, 1999.

[19] F.L. Lewis. 'Optimal Control'. New York: Wiley, 1986.

[20] S. Haykin. 'Neural Networks: A comprhensive foundation'. Prentice-Hall, 1999.

Appendix A - Equivalence of the HCW equations and the hamiltonian equations of motion

For the purposes of this proof, the z component is not considered as it is decoupled and trivial to prove. The HCW equations of motion are:

$$\begin{aligned} &\ddot{x} - 2\dot{\theta}\dot{y} - \ddot{\theta}y - \dot{\theta}^2 x - 2\frac{\mu}{r^3}x = 0 \\ &\ddot{y} + 2\dot{\theta}\dot{x} + \ddot{\theta}x - \dot{\theta}^2 y + \frac{\mu}{r^3}y = 0 \end{aligned} \tag{12.1}$$

The Hamiltonian equations of motion equivalent to (12.1) are:

$$\begin{aligned} \dot{x} &= p_x + \dot{\theta}y - \dot{r} \\ \dot{y} &= p_y - \dot{\theta}(r + x) \\ \dot{p}_x &= -\frac{\mu}{r^2} + \frac{2\mu x}{r^3} + p_y\dot{\theta} \\ \dot{p}_y &= -\frac{\mu y}{r^3} - \dot{\theta}p_x \end{aligned} \tag{12.2}$$

differentiating $\dot{x} = p_x + \dot{\theta}y - \dot{r}$ gives

$$\ddot{x} = \dot{p}_x + \ddot{\theta}y + \dot{\theta}\dot{y} - \ddot{r} \tag{12.3}$$

substituting $\dot{p}_x = -\frac{\mu}{r^2} + \frac{2\mu x}{r^3} + p_y\dot{\theta}$ into equation (12.3) gives

$$\ddot{x} = -\frac{\mu}{r^2} + \frac{2\mu x}{r^3} + p_y\dot{\theta} + \ddot{\theta}y + \dot{\theta}\dot{y} - \ddot{r} \tag{12.4}$$

then from the equations for the canonical momenta substituting $p_y = r\dot{\theta} + x\dot{\theta} + \dot{y}$ into equation (12.4) gives

$$\ddot{x} = -\frac{\mu}{r^2} + \frac{2\mu x}{r^3} + (r\dot{\theta} + x\dot{\theta} + \dot{y})\dot{\theta} + \ddot{\theta}y + \dot{\theta}\dot{y} - \ddot{r} \tag{12.5}$$

Simplifying and rearranging (12.5) yields:

$$\ddot{x} - 2\dot{\theta}\dot{y} - \ddot{\theta}y - \dot{\theta}^2 x - \frac{2\mu x}{r^3} + \ddot{r} + \frac{\mu}{r^2} - r\dot{\theta}^2 = 0 \tag{12.6}$$

The 2nd order equation of the radius of an ideal Keplerian orbit is

$$\ddot{r} + \frac{\mu}{r^2} - r\dot{\theta}^2 = 0 \tag{12.7}$$

Thus, equation (12.6) becomes

$$\ddot{x} - 2\dot{\theta}\dot{y} - \ddot{\theta}y - \dot{\theta}^2 x - \frac{2\mu x}{r^3} = 0 \tag{12.8}$$

this is the form of the equation in (12.1). The second equation in (12.1) in y is derived in the same manner. Differentiating

$$\dot{y} = p_y - \dot{\theta}(r + x) \tag{12.9}$$

gives

$$\ddot{y} = \dot{p}_y - \ddot{\theta}r - \ddot{\theta}x - \dot{\theta}\dot{r} - \dot{\theta}\dot{x} \tag{12.10}$$

then substituting $p_x = \dot{r} + \dot{x} - \dot{\theta}y$ into

$$\dot{p}_y = -\frac{\mu y}{r^3} - \dot{\theta}p_x \tag{12.11}$$

and substituting (12.11) into equation (12.10) gives

$$\ddot{y} = -\frac{\mu y}{r^3} - \dot{\theta}(\dot{r} + \dot{x} - \dot{\theta}y) - \ddot{\theta}r - \ddot{\theta}x - \dot{\theta}\dot{r} - \dot{\theta}\dot{x} \tag{12.12}$$

Rearranging and simplifying (12.12) yields:

$$\ddot{y} + 2\dot{\theta}\dot{x} + \ddot{\theta}x - \dot{\theta}^2 y + \frac{\mu}{r^3}y + \ddot{\theta}r + 2\dot{\theta}\dot{r} = 0 \tag{12.13}$$

The 2nd order differential equation in θ for an ideal Keplarian orbit is

$$\ddot{\theta}r + 2\dot{\theta}\dot{r} = 0 \tag{12.14}$$

therefore equation (12.13) equates to:

$$\ddot{y} + 2\dot{\theta}\dot{x} + \ddot{\theta}x - \dot{\theta}^2 y + \frac{\mu}{r^3}y = 0 \tag{12.15}$$

which is the equation in y in (12.1). Therefore the two sets of equations (12.1) and (12.2) are equivalent.

Appendix B - The study model

The study model below are the Hamiltonian canonical equations of relative motion calculated using the equations (3.11) and include eccentricity, nonlinear gravitational terms and $H^{(1)}$ the J_2 perturbation. These equations were computed using Mathematica:

$$
\begin{aligned}
\dot{x} &= p_x + \dot{\theta} y - \dot{r} \\
\dot{y} &= p_y - \dot{\theta}(r + x) \\
\dot{z} &= p_z \\
\dot{p}_x &= p_y \dot{\theta} - \frac{\mu(r+x)}{((r+x)^2 + y^2 + z^2)^{1/2}} - \frac{3J_2 R_e^2 \mu (r+x)((r+x)^2 + y^2 - 4z^2)}{2((r+x)^2 + y^2 + z^2)^{7/2}} \\
\dot{p}_y &= -p_x \dot{\theta} - \frac{\mu y}{((r+x)^2 + y^2 + z^2)^{1/2}} - \frac{3J_2 R_e^2 y \mu (r+x)((r+x)^2 + y^2 - 4z^2)}{2((r+x)^2 + y^2 + z^2)^{7/2}} \\
\dot{p}_z &= -\frac{\mu z}{((r+x)^2 + y^2 + z^2)^{1/2}} - \frac{9J_2 R_e^2 z \mu ((r+x)^2 + y^2 - 2z^2)}{2((r+x)^2 + y^2 + z^2)^{7/2}}
\end{aligned}
\tag{12.16}
$$

Appendix C - The full model

The full model of relative motion is calculated using the equations (3.11) and include eccentricity, nonlinear gravitational terms and $H^{(1)}$ the J_2 perturbation, air drag and actuation parameters. These equations were computed using Mathematica:

$$
\begin{aligned}
&\dot{x} = p_x + \dot{\theta} y - \dot{r} \\
&\dot{y} = p_y - \dot{\theta}(r + x) \\
&\dot{z} = p_z \\
&\dot{p}_x = p_y \dot{\theta} - \frac{\mu(r + x)}{((r + x)^2 + y^2 + z^2)^{1/2}} - \frac{3J_2 R_e^2 \mu(r + x)((r + x)^2 + y^2 - 4z^2)}{2((r + x)^2 + y^2 + z^2)^{7/2}} \\
&+u_x \\
&\dot{p}_y = -p_x \dot{\theta} - \frac{\mu y}{((r + x)^2 + y^2 + z^2)^{1/2}} - \frac{3J_2 R_e^2 y \mu(r + x)((r + x)^2 + y^2 - 4z^2)}{2((r + x)^2 + y^2 + z^2)^{7/2}} \\
&+u_y \\
&\dot{p}_z = -\frac{\mu z}{((r + x)^2 + y^2 + z^2)^{1/2}} - \frac{9J_2 R_e^2 z \mu((r + x)^2 + y^2 - 2z^2)}{2((r + x)^2 + y^2 + z^2)^{7/2}} \\
&+u_z
\end{aligned}
\tag{12.17}
$$

where $[u_x, u_y, u_z]$ are the actuation signals.